

Positronium–Proton Scattering at Low Energies

Jim Mitroy

Faculty of Science, Northern Territory University,
Casuarina, NT 0909, Australia.

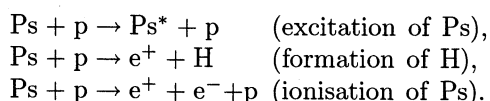
Abstract

Calculations of low energy positronium–proton scattering using the close coupling approach are reported at energies below the three-body breakup energy of 0.5 Rydberg. The channel space includes nine physical hydrogen and positronium states and in addition twelve hydrogen and positronium pseudo-states. Total elastic and electron-transfer cross sections are reported at incident energies below the ionisation threshold. Cross sections for electron transfer to the $H(n=2)$ and $H(n=3)$ levels are also reported.

1. Introduction

The combination of (e^-e^+p) is one of the fundamental three-body systems of atomic physics. As a three-body system, it does not possess a stable bound state, but there are two-particle bound states that can be formed from its constituents. These are the hydrogen atom, which is stable, and the positronium atom which has a lifetime of about 10^{-6} s before undergoing positron–electron annihilation. Because of this, the positron–hydrogen and positronium–proton collision systems form one of the simplest possible scattering systems in which a genuine rearrangement collision is possible. While there have recently been a number of calculations of positron–hydrogen scattering (Archer *et al.* 1990; Hewitt *et al.* 1990; Higgins and Burke 1993; Igarashi and Toshima 1994; McAlinden *et al.* 1994; Mitroy and Stelbovics 1994*a*, 1994*b*; Mitroy and Ratnavelu 1995; Roy and Mandal 1993; Zhou *et al.* 1994), the same cannot be said for positronium–proton scattering. This is despite the fact that the behaviour of the positronium–proton elastic phase shift is quite unusual at high energies (Mitroy *et al.* 1995), and the positronium–antiproton to electron–antihydrogen reaction has been promoted as one of the most efficient ways to form antihydrogen (Charlton *et al.* 1994; Deutch *et al.* 1988, 1993).

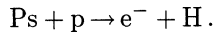
The following events are possible in a positronium–proton collision:



The present close coupling (CC) calculations of positronium–proton scattering are restricted to energies below the three-body breakup threshold. The channel

space includes a total of thirteen hydrogen-type states and a total of eight positronium-type states, including the exact $H(n=1, 2, 3)$ and $Ps(n=1, 2)$ states, and is identical to a previous calculation of positron–hydrogen scattering (Mitroy 1995). Indeed, for the most part, the T -matrix elements used for the computation of the present cross sections are taken from the T -matrix files generated during the positron–hydrogen calculations. The present calculations are only possible because an efficient technique for computing the electron-transfer matrix elements used in the momentum space T -matrix method has been developed (Mitroy 1993*a*).

Most of the earlier calculations of Ps–p scattering (Darewych 1987; Humberston *et al.* 1987; Nahar and Wadehra 1988; Mitroy and Stelbovics 1994*b*; Igarashi *et al.* 1994) were prompted by a desire to compute anti-hydrogen cross sections for the reaction



The only comprehensive calculations of Ps–p scattering reported so far have been the six-state CC calculation by Mitroy and Stelbovics (1994*a*) and the more accurate twelve-state CC calculation by Mitroy and Ratnavelu (1995). There has been one other calculation reporting cross sections for Ps–p scattering (Archer *et al.* 1990), however this calculation was restricted to the $J = 0$ partial wave.

2. Details of the Calculations

The primary purpose of the calculations reported in this paper is to generate accurate cross sections for positronium–proton scattering in the low energy region. The cross sections reported in this paper are for the most part derived from T -matrix elements generated from earlier calculations. Under these circumstances, a detailed description of the computational procedures is not required, although the more important details are summarised. The three model calculations for which cross sections are reported are:

CC(3, 3). This basis includes the physical $H(1s)$, $H(2s)$ and $H(2p)$, and $Ps(1s)$, $Ps(2s)$ and $Ps(2p)$ levels. This basis entailed no new calculations since cross sections and phase shifts have been reported previously (Mitroy and Stelbovics 1994*a*).

CC($\bar{6}$, $\bar{6}$). This basis includes the lowest three physical levels of hydrogen (1s, 2s and 2p) and well as three pseudo-levels ($\bar{3s}$, $\bar{3p}$ and $\bar{3d}$). The lowest three physical states of positronium (1s, 2s and 2p) and three pseudo-positronium levels ($\bar{3s}$, $\bar{4s}$ and $\bar{3p}$) were included. Extensive calculations with this basis have been reported previously (Mitroy 1993*b*; Mitroy and Ratnavelu 1995).

CC($\bar{13}$, $\bar{8}$). This basis includes the lowest six physical levels of hydrogen (1s, 2s, 2p, 3s, 3p, 3d) and well as seven pseudo-levels ($\bar{4s}$, $\bar{5s}$, $\bar{4p}$, $\bar{5p}$, $\bar{6p}$, $\bar{4d}$, $\bar{4f}$). The lowest three physical states of positronium (1s, 2s 2p) and five pseudo-positronium levels were included ($\bar{3s}$, $\bar{4s}$, $\bar{3p}$, $\bar{4p}$ and $\bar{3d}$). The detailed specification of this basis has been given elsewhere (Mitroy 1995). Calculations at some additional energies have been performed.

For most of the calculations reported in this paper, 40 and 48 point Gaussian quadrature meshes were used to discretise the kernel of the integral equation. Calculations were done at more than 200 energies below the $Ps(n=3)$ threshold

to properly map out the resonance structures associated with the $H(n=2)$ and $Ps(n=2)$ thresholds. Some complicated structures exist between the $Ps(n=2)$ and $H(n=3)$ thresholds (Archer *et al.* 1990). There has been no attempt to investigate this particular energy region in any detail since this necessitates increasing the size of the Gaussian mesh used to discretise the integral equation. Calculations were only performed at four energies above the $H(n=3)$ threshold.

Since the time taken to evaluate the positronium matrix elements increased for the higher partial waves, the fully coupled $CC(\overline{13}, \overline{8})$ model was not used for all the partial waves. For the lowest partial waves no approximations (apart from the purely numerical ones inherent in any calculation) were made to compromise the accuracy of the $CC(\overline{13}, \overline{8})$ calculations. For an intermediate set of J -values, the matrix elements connecting the hydrogen states to the positronium states were omitted and the two manifolds were decoupled from each other. For the highest partial waves, a modified effective range formula (MERT) (Mitroy and Ratnavelu 1995; O'Malley *et al.* 1962; O'Malley 1963) was used to compute the approximate T -matrix elements for the diagonal channels. The MERT approximation to the phase shift is

$$\tan\delta_J = \frac{2\pi\alpha_d(Ps)k^2}{(2J+3)(2J+1)(2J-1)}. \quad (1)$$

[An earlier expression given by Mitroy and Ratnavelu (1995) had a typographical error and was a factor of 2 too large.] However, it was possible to ensure that the use of these approximations would not lead to an inaccuracy of more than 1% in the integrated cross sections by checking the accuracy of the different approximations at the changeover J -values.

3. Elastic Scattering

One of the salient features of $Ps(1s)$ - p scattering is that the $e^+H(1s)$ channel is also open. This results in the phase shifts for elastic scattering having both real and imaginary components. Another unusual aspect is that the $Ps(1s) + p \rightarrow e^+ + H(1s)$ reaction is a superelastic collision. One consequence of the superelastic nature of the transition is that the electron transfer cross section will asymptote like $E^{-\frac{1}{2}}$ at threshold, where E is the energy in the $Ps(1s)$ - p entrance channel (Mott and Massey 1965; Mitroy and Stelbovics 1994; McAlinden *et al.* 1994). Another exotic effect is a consequence of the fact that positron and electron have the same mass, and therefore the centre-of-mass and centre-of-charge of the positronium atom are coincident. The static interaction between a proton and a positronium atom will be zero, and so the first Born approximation to the elastic scattering T -matrix element is zero (Massey and Mohr 1954; Mitroy 1993*a*, 1993*b*). Consequently, elastic scattering can only occur as a result of second order or higher order processes.

Both the real (Fig. 1) and imaginary (Fig. 2) parts of the phase shift are graphed for the $J=0$, $J=1$ and $J=2$ partial waves. Comparison of the $CC(\overline{13}, \overline{8})$ and $CC(\overline{6}, \overline{6})$ phase shifts reveals that the $CC(\overline{13}, \overline{8})$ phase shifts are larger as expected. The differences between the $CC(\overline{13}, \overline{8})$ and $CC(\overline{6}, \overline{6})$ sets of phase shifts are not large, being less than 5% at most energies. The six-state $CC(3,3)$ model provides a poor approximation to these more accurate calculations. For the $J=0$

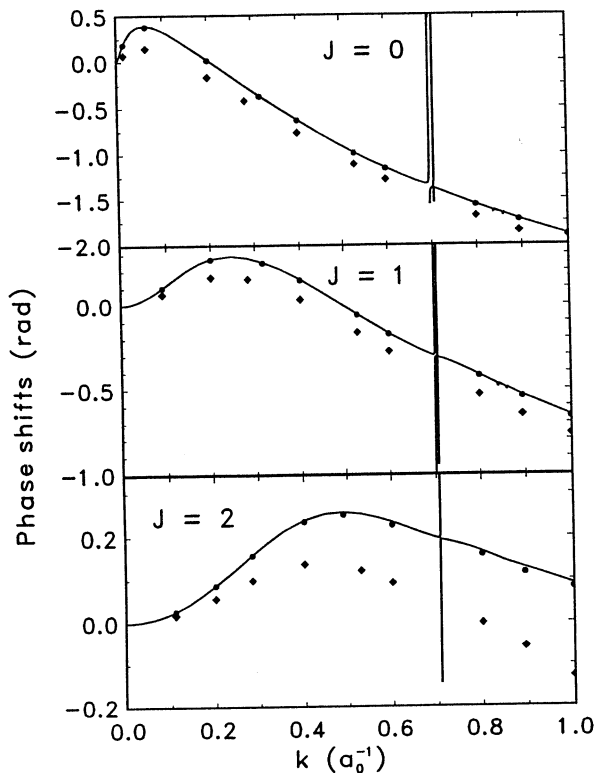


Fig. 1. Real part of the $J = 0, 1$ and 2 phase shifts (—). Phase shifts from the $CC(\bar{6}, \bar{6})$ (●) and $CC(3, 3)$ (◆) models are also shown.

and 1 partial waves, the differences are greater than 0.1 rad at most energies. The differences between the $CC(3,3)$ and $CC(\bar{13}, \bar{8})$ phase shifts are larger for the $J = 2$ partial wave. However, the dipole polarisability for the positronium ground state is quite large at $36.0 a_0^3$, so any deficiencies in the polarisation potential will be emphasised. The $CC(3, 3)$ basis takes into account only 65.8% of the positronium ground state polarisability. Another factor that accentuates the influence of the polarisation potential is the fact that the first-order contribution to the elastic scattering T -matrix is zero.

The scattering length for Ps-p scattering was estimated by fitting a MERT formula (O'Malley *et al.* 1962; O'Malley 1963) to six values of the s-wave phase between 0.0141 and $0.07 a_0^{-1}$. (When performing the fit, the effective dipole polarisability that is used in the MERT formula is $72 a_0^3$.) The present scattering length is $-15.5 \pm 0.4 a_0$. The error bar provides an estimate of the uncertainty from the MERT fit, and should not be taken as giving an absolute bound on the scattering length. Mitroy and Ratnavelu (1995) previously estimated the scattering length to be $-16 a_0$ for the $CC(\bar{6}, \bar{6})$ model using a graphical technique. A better estimate of the $CC(\bar{6}, \bar{6})$ scattering length, namely $-15.2 \pm 0.4 a_0$, was obtained using a MERT fit. Using the present value for the scattering length would imply an elastic cross section of $960 \pi a_0^2$ at threshold.

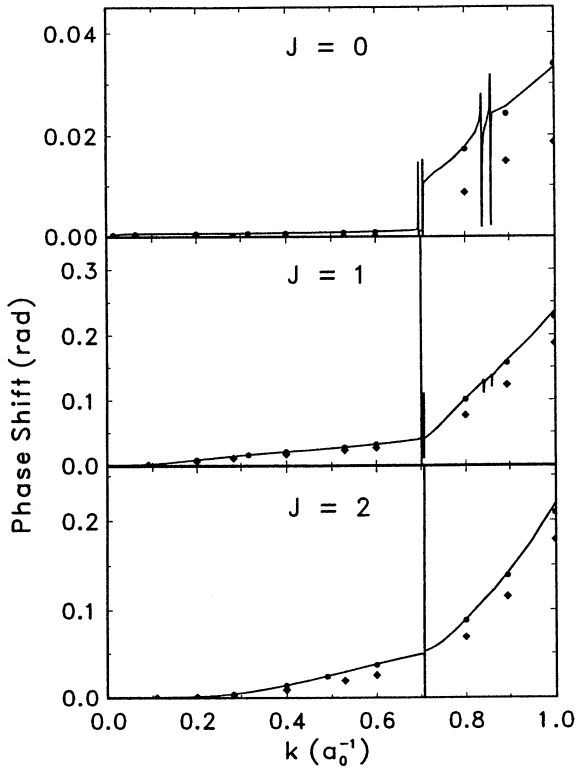


Fig. 2. Imaginary part of the $J = 0, 1$ and 2 phase shifts (—). Phase shifts from the $CC(\bar{6}, \bar{6})$ (●) and $CC(3, 3)$ (◆) models are also shown.

One of the features of the plots shown in Fig. 1 is that the $J = 0$ and $J = 1$ phase shifts both pass through zero at momenta of 0.207 and $0.49 a_0^{-1}$ respectively. It would be necessary to extend the calculation to higher energies to determine whether the $J = 2$ phase also goes through zero. Although minima are present in the $J = 0$ and $J = 1$ cross sections (Fig. 3), these occur at different energies and as a consequence there is no pronounced Ramsauer minimum in the integrated elastic cross section (Fig. 4).

The imaginary phase shift provides a measure of the loss of flux from the $Ps(1s)$ - p entrance channel. One notable feature of Fig. 2 is the manner in which the imaginary phase shift increases as a function of energy. At the $H(2s)$ and $H(2p)$ thresholds ($k \sim 0.7 a_0^{-1}$) the rate of increase of the imaginary phase shift gets larger. This can be interpreted as reflecting the fact that the transitions to form hydrogen in the $H(2s)$ and $H(2p)$ levels are stronger than the transition to the $H(1s)$ level.

There are resonances associated with both the $H(n=2)$ and $Ps(n=2)$ thresholds. The real part of the phase shifts all increase by π when going through the $H(n=2)$ resonances. The resonances associated with $Ps(n=2)$ threshold lead to structures in the real part of the phase shift which are barely perceptible although there are prominent features in the imaginary part of the phase shift for the $J = 0$ partial wave.

The elastic cross sections for the $J = 0, 1, 2$ and 3 partial waves are listed in Table 1 and a detailed plot of the $J = 0, 1$ and 2 partial cross sections is shown in Fig. 3. The differences between the $CC(\bar{6}, \bar{6})$ and $CC(\bar{13}, \bar{8})$ cross sections are less than 10% at all the energies detailed in Table 1.

Table 1. The $J = 0, 1, 2$ and 3 partial cross sections (in units of πa_0^2) for Ps(1s)-p elastic scattering

The integrated cross sections are also given

Model	Energy (Ryd)						
	0.0041	0.0625	0.14	0.2225	0.300	0.400	0.5000
$J = 0$							
CC(3, 3) ^a	6.53	11.1	11.5	8.80	6.54	4.49	3.15
CC($\bar{6}, \bar{6}$) ^b	56.4	7.07	9.92	8.34	6.45	4.64	3.35
CC($\bar{13}, \bar{8}$)	59.7	6.92	9.86	8.32	6.45	4.64	3.37
Variational ^c	56.7	7.05	9.93	8.37			
$J = 1$							
CC(3, 3) ^a	5.85	0.784	1.11	3.40	4.12	4.50	4.25
CC($\bar{6}, \bar{6}$) ^b	15.0	3.97	0.181	1.82	2.56	3.22	3.29
CC($\bar{13}, \bar{8}$)	15.2	4.17	0.160	1.77	2.51	3.14	3.22
$J = 2$							
CC(3, 3) ^a	0.336	2.55	1.03	0.184	0.102	0.333	0.656
CC($\bar{6}, \bar{6}$) ^b	0.785	6.86	4.07	1.71	0.962	0.619	0.670
CC($\bar{13}, \bar{8}$)	0.792	7.07	4.26	1.82	1.03	0.683	0.729
Variational ^c	0.0021	4.68	2.82	0.697			
$J = 3$							
CC(3, 3) ^a	0.0487	0.799	1.271	1.24	1.18	0.875	0.701
CC($\bar{6}, \bar{6}$) ^b	0.113	1.82	3.18	3.46	3.39	2.71	2.13
CC($\bar{13}, \bar{8}$)	0.119	1.85	3.32	3.64	3.56	2.85	2.25
Total							
CC(3, 3) ^a	12.8	15.6	15.7	14.9	13.8	12.2	11.0
CC($\bar{6}, \bar{6}$)	72.7	20.5	19.2	18.3	17.6	16.3	14.6
CC($\bar{13}, \bar{8}$)	75.9	20.8	19.5	18.6	18.0	16.7	15.0

^a Mitroy and Stelbovics (1994b).

^b Mitroy and Ratnavelu (1995).

^c Humberston (1984), Brown and Humberston (1984) (cross sections derived from the K -matrix elements).

Elastic cross sections for the $J = 0$ and $J = 2$ partial waves have also been derived from the variational K -matrix elements of Humberston (1984) and Brown and Humberston (1985). [In Mitroy and Ratnavelu (1995), the cross sections attributed to Humberston and Brown were computed from the real part of the phase shift and are slightly different.] The variational cross sections for $J = 0$ are in reasonable agreement with the close coupling calculations, although they are in better agreement with the $CC(\bar{6}, \bar{6})$ calculation. For $J = 2$, the variational cross sections are in poor agreement with the present cross section. Since it is not clear whether Humberston and Brown were interested in getting accurate cross sections for the Ps(1s)-p entrance channel, it is probably to be expected that their cross sections for the Ps(1s)-p entrance channel are not of the same high quality as their cross sections for the positron-hydrogen entrance channel. Since they do not report their K -matrix elements for $J = 1$, it is not possible to make a

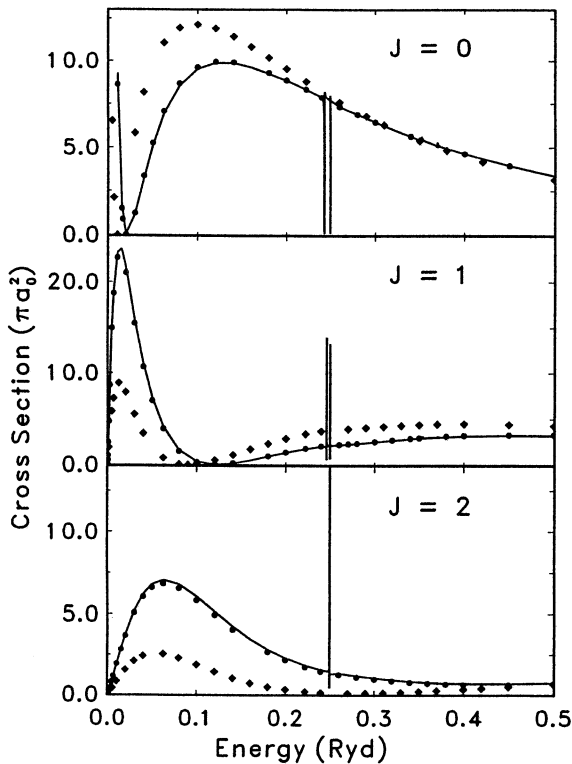


Fig. 3. Elastic scattering cross sections (in πa_0^2) for the $J = 0, 1$ and 2 partial waves (—). Partial cross sections from the $CC(3, 3)$ and (\blacklozenge) and $CC(\bar{6}, \bar{6})$ (\bullet) models are also shown.

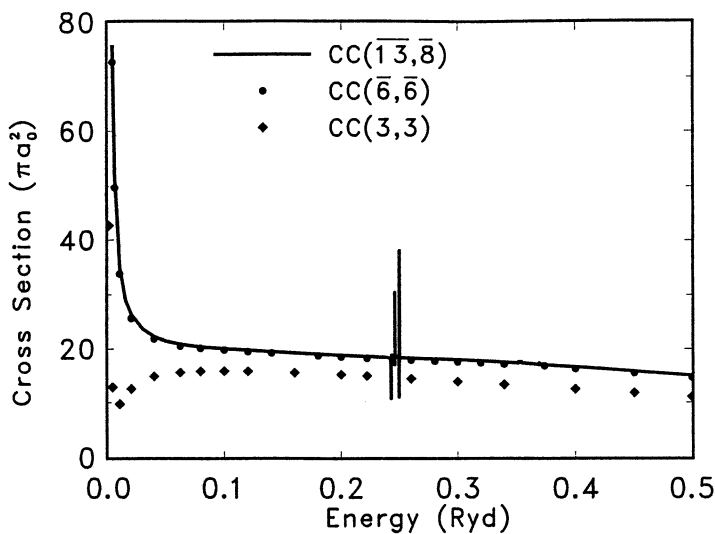


Fig. 4. Elastic cross section (in πa_0^2) for positronium-proton scattering at energies below the three-body ionisation threshold. Besides the $CC(\bar{13}, \bar{8})$ calculation, cross sections from the $CC(3, 3)$ (\blacklozenge) and $CC(\bar{6}, \bar{6})$ (\bullet) models are shown.

comparison in this case. We suspect that the poor results obtained for $J = 2$ may reflect the use of trial functions that were not particularly suitable for describing the strong polarisation interactions present in the Ps(1s)-p entrance channel.

The last rows of Table 1 list the integral cross section for a number of different calculations. The CC(3,3) model provides a relatively poor description of positronium-proton scattering. Although the difference between the CC(3,3) and CC($\overline{13}$, $\overline{8}$) cross sections is only $4\pi a_0^2$ at an incident energy of 0.5 Ryd, the CC(3,3) and the CC($\overline{13}$, $\overline{8}$) phase shifts have the opposite sign. Under these circumstances, a difference of only $4\pi a_0^2$ between the CC(3,3) and CC($\overline{13}$, $\overline{8}$) cross sections can be regarded as fortuitous. The differences between the CC($\overline{6}$, $\overline{6}$) and CC($\overline{13}$, $\overline{8}$) cross sections are less than 5%, and give an indication of the overall convergence of the CC($\overline{13}$, $\overline{8}$) cross sections. The integrated cross section is plotted in Fig. 4. The two salient features of the integrated elastic cross section are the large size of the cross section at threshold and the featureless nature of the cross section for incident Ps energies >0.1 Ryd. The resonant features near the H($n=2$) and Ps($n=2$) thresholds are very narrow (Mitroy 1995).

4. Charge Transfer Cross Section to form Hydrogen

The electron-transfer reaction to form antihydrogen is a superelastic collision and the s-wave partial cross section can be expected to diverge like $E^{-\frac{1}{2}}$ as $E \rightarrow 0$. This is visible in Fig. 5 where the $J = 0$ cross section for electron transfer to the H(1s) state is depicted. A detailed tabulation of the partial cross sections has not been provided, since this information can be derived from Table 2 of Mitroy (1995) by using the principle of detailed balance. Instead, total cross sections for transitions to the different final hydrogen states are given in Tables 2 and 3.

Table 2. Integrated cross sections (in πa_0^2) for hydrogen formation in the H(1s) ground state

Model	Energy (Ryd)						
	0.0041	0.0625	0.14	0.2225	0.30	0.40	0.50
CC(3,3) ^a	1.099	2.38	2.74	2.94	2.90	2.76	2.55
CC($\overline{6}$, $\overline{6}$) ^b	1.870	3.24	3.74	3.99	3.89	3.66	3.37
CC($\overline{13}$, $\overline{8}$)	1.924	3.28	3.79	4.05	3.95	3.71	3.40
Hyper ^c		3.34	3.82	4.06	3.97	3.70	3.39

^a Mitroy and Stelbovics (1994b).

^b Mitroy and Ratnavelu (1995).

^c Hyperspherical CC, Igarashi *et al.* (1994).

The $J = 0, 1$ and 2 partial cross sections for electron transfer to the H(1s) state are depicted in Fig. 5. The trends noticed in the discussion of the elastic cross sections are also present for the electron transfer cross sections. The differences between the CC($\overline{6}$, $\overline{6}$) and CC($\overline{13}$, $\overline{8}$) cross sections are uniformly small for all the partial waves. On the other hand, the CC(3,3) model gives cross sections which are quite different from the CC($\overline{13}$, $\overline{8}$) cross sections.

The integrated cross sections for H-formation in the H(1s) ground state are depicted in Fig. 6 and the cross sections for H-formation in the H(2s) and H(2p) levels are shown in Fig. 7. The differences between the CC($\overline{6}$, $\overline{6}$) and CC($\overline{13}$, $\overline{8}$) cross sections for H-formation in the 1s state are less than 3% at most energies. Similarly, the hyperspherical close coupling calculation of Igarashi *et al.* (1994)

gives cross sections which are very close to the $CC(\overline{13}, \overline{8})$ calculation. It should be noted that the cross sections Igarashi *et al.* tabulated in Tables 2 and 3 were not computed at exactly the same energies at the present cross section. However, the differences in energy are sufficiently small (~ 0.003 Ryd) that a direct comparison is possible.

Table 3. Integrated cross sections (in πa_0^2) for hydrogen formation in the H(2s), H(2p), H(3s), H(3p) and H(3d) levels

Model	Energy (Ryd)		
	0.30	0.40	0.50
	H(2s)		
CC(3, 3) ^a	0.889	1.32	1.38
CC($\overline{6}, \overline{6}$) ^b	1.125	1.66	1.82
CC($\overline{13}, \overline{8}$)	1.187	1.74	1.94
Hyper ^c	1.15	1.94	2.19
	H(2p)		
CC(3, 3) ^a	2.90	6.36	8.84
CC($\overline{6}, \overline{6}$) ^b	3.08	6.71	9.13
CC($\overline{13}, \overline{8}$)	3.25	6.91	9.50
Hyper ^c	2.72	6.88	9.41
	H(3s)		
CC($\overline{13}, \overline{8}$)		0.0229	0.0989
Hyper ^c		0.0434	0.0720
	H(3p)		
CC($\overline{13}, \overline{8}$)		0.0580	0.178
Hyper ^c		0.0930	0.224
	H(3d)		
CC($\overline{13}, \overline{8}$)		0.0445	0.427
Hyper ^c		0.0459	0.397

^aMitroy and Stelbovics (1994b).

^bMitroy and Ratnavelu (1995).

^cHyperspherical CC, Igarashi *et al.* (1994).

The differences between the calculations are larger for H-formation in the H(2s) and the H(2p) states. The cross sections for the H($n=2$) levels are more sensitive to the larger basis sizes used in the $CC(\overline{13}, \overline{8})$ and hyperspherical calculations. The more primitive CC(3, 3) model does a reasonable job of reproducing the H(2p) formation cross section, although it is less accurate for the H(1s) and H(2s) cross sections. The total H-formation cross section obtained by summing the H-formation cross sections to all the individual levels are also shown in Fig. 6. The inclusion of the H($n=3$) levels serves to enhance the differences between the $CC(\overline{6}, \overline{6})$ and $CC(\overline{13}, \overline{8})$ models for positronium energies > 0.4 Ryd. The $CC(\overline{6}, \overline{6})$ basis does not include these states which contribute a total of $0.7 \pi a_0^2$ to the electron transfer cross section at 1.0 Ryd.

The present cross sections for hydrogen formation can be related to the cross section for antihydrogen formation

$$\text{Ps}(1s) + \bar{p} \rightarrow e^- + \bar{\text{H}}(n'l'),$$

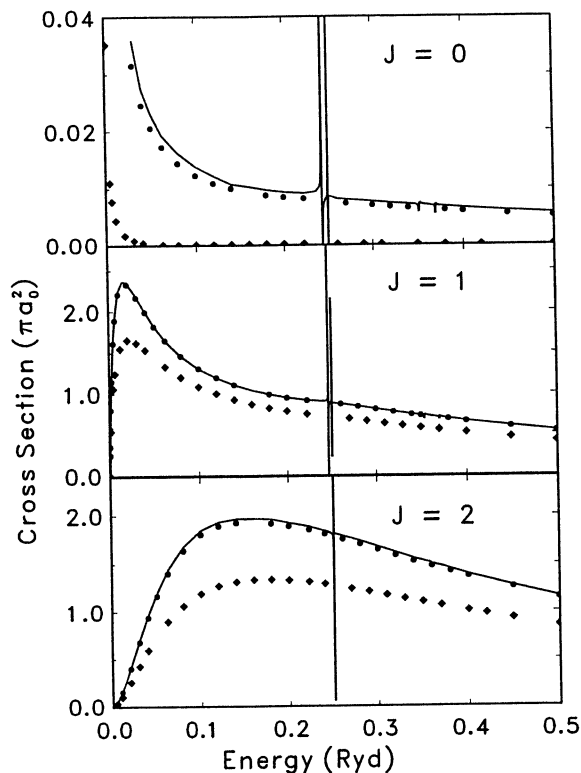


Fig. 5. The $J = 0, 1$ and 2 partial cross sections (in πa_0^2) for the $\text{Ps}(1s)+p \rightarrow e^+\text{H}(1s)$ reaction (—). Cross sections from the $\text{CC}(\bar{6}, \bar{6})$ (\bullet) and $\text{CC}(3, 3)$ (\blacklozenge) models are also shown.

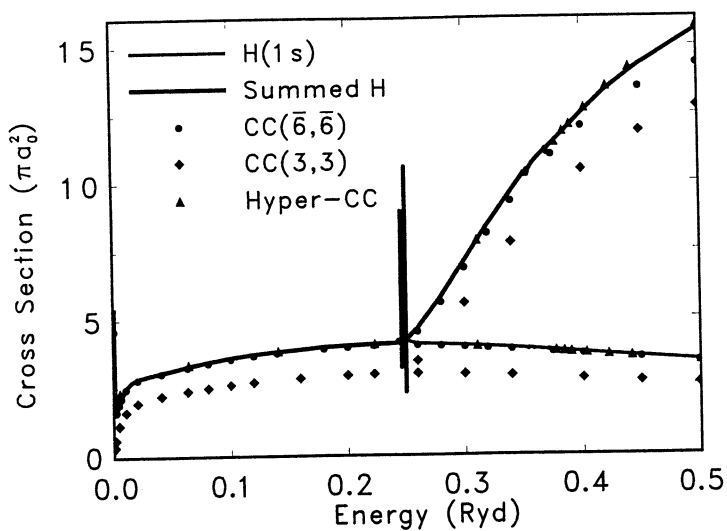


Fig. 6. Cross sections (in πa_0^2) for hydrogen formation in its ground state via the reaction $\text{Ps}(1s)+p \rightarrow e^+\text{H}(1s)$. Also shown is the total hydrogen formation cross section which includes H formation in the $n = 1, 2$ and 3 levels. The cross sections from the $\text{CC}(\bar{6}, \bar{6})$ (\bullet) and $\text{CC}(3, 3)$ (\blacklozenge) models are shown along with those from the hyperspherical CC calculations of Igarashi *et al.* (1994) (\blacktriangle).

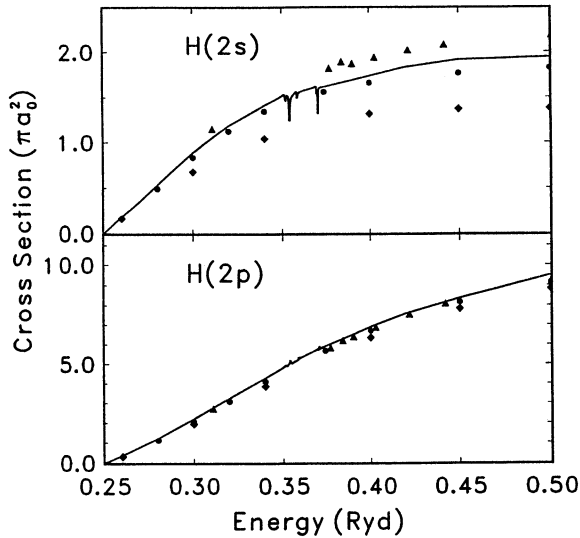


Fig. 7. Cross sections (in πa_0^2) for hydrogen formation in the H(2s) and H(2p) states by the electron-transfer reaction (—). The cross sections from the CC($\bar{6}, \bar{6}$) (●) and the CC(3, 3) (◆) models are shown along with those from the hyperspherical CC calculations of Igarashi *et al.* (1994) (▲).

by charge conjugation symmetry. The cross sections that are most relevant to proposed experiments to form antihydrogen (Deutch *et al.* 1988, 1993; Charlton *et al.* 1994) are those shown in Fig. 6. Since it is likely that the first attempt to form antihydrogen will involve collisions with the positronium ground state at thermal energies of about 1 eV, the cross sections that are most relevant are those at about 0.1 Ryd. A larger collision energy would lead to an increased antihydrogen production rate. But it is unlikely that the relative collision energy can be increased in the cryogenic traps that will be used in the initial attempts to form antihydrogen.

Given that the most important application of the present work is to the calculation of antihydrogen formation cross sections, the overall degree of consistency that exists between the C($\bar{6}, \bar{6}$), CC($\bar{13}, \bar{8}$) and hyperspherical calculation of Igarashi *et al.* (1994) means that for all practical purposes the calculation of the electron (positron) transfer cross section from the Ps ground state at low energies can be regarded as a solved problem.

5. Total Reaction Cross Section

The total reaction cross section for Ps(1s)-p scattering is shown in Fig. 8. In order to simplify the analysis, the contributions to the cross section are collected into two components, the elastic and positronium excitation transitions, and those involving the transfer of an electron to form hydrogen. For most of the energy range the dominant contribution to the total cross section comes from the elastic cross section (the Ps-excitation cross sections are small). It is only at 1.0 Ryd that the H-formation cross section becomes comparable in size to the elastic cross section.

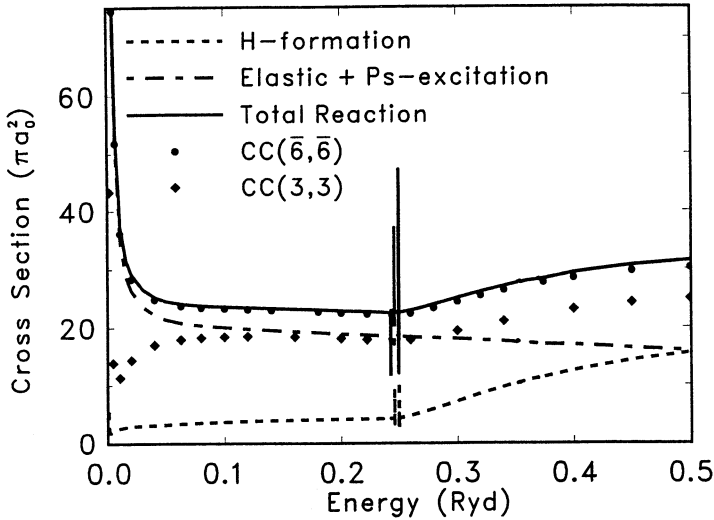


Fig. 8. Total reaction cross section (in πa_0^2) for positronium-proton scattering (—). The separate contributions to the cross section from electron-transfer and non-electron-transfer reactions are shown. The total reaction cross sections from the $CC(\bar{6}, \bar{6})$ (●) and $CC(3, 3)$ (◆) calculations are also displayed.

The close comparison with the $CC(\bar{6}, \bar{6})$ cross section indicates that the present $CC(\bar{13}, \bar{8})$ cross section is close to convergence. The $CC(\bar{13}, \bar{8})$ cross section includes the possibility of electron transfer to the $H(n=3)$ levels which are of course not included in the $CC(\bar{6}, \bar{6})$ calculation. Since the cross sections for excitation to the $Ps(n=2)$ states and electron transfer to the $H(n=3)$ states are 0.9 and $0.7 \pi a_0^2$ respectively, the omission of the higher Ps and H states from the calculation are not expected to result in a major error in the total cross section. Accordingly, a conservative estimate of the accuracy of the present total cross section would be that the non-resonant part of the total reaction cross section would be accurate to better than 10%. The present total cross section should be most accurate at low energies and least accurate at energies close to the ionisation threshold.

6. Conclusions

A set of cross sections for $Ps(1s)$ - p scattering has been computed with a 21 state close coupling calculation. The present cross sections supersede those computed earlier in the framework of a 12-state calculation (Mitroy and Ratnavelu 1995) and represent the best that have so far been computed. They should be regarded as providing the benchmark for future calculations. Comparisons with the earlier 12-state calculation would indicate that the overall accuracy of the integrated cross sections reported in this work should be better than 10%.

An accurate estimate of the scattering length has been obtained and the scattering length is seen to be large in magnitude ($-15.5 \pm 0.4 a_0$). This results in the elastic cross section having a threshold value of $960 \pi a_0^2$. The probable

cause for the large value of the elastic cross section at threshold and higher energies is the strong polarisation potential.

It would not be worth while to try and extend the size of the present calculation and extend the calculation into the intermediate energy region without radically changing the method of basis selection. The $\text{Ps}(1s)+p \rightarrow \text{Ps}(2p)+p$ cross sections from an 18-state R -matrix calculation by Kernoghan *et al.* (1994) exhibited a great deal of structure above the ionisation threshold. Since these structures are most likely spurious, it seems likely that an enlarged basis would only lead to pseudo-structures even more complicated than those found by Kernoghan *et al.* (1994). A more promising approach would be to try and increase either the hydrogen-type or positronium-type basis to completeness using L^2 techniques while retaining a few levels of the other type in the CC expansion. Numerical instabilities associated with an over-complete basis (Bransden and Noble 1994; Mitroy 1995) would make it impractical to simultaneously increase the size of both the hydrogen and positronium channel spaces to completeness.

Acknowledgments

The calculations reported in this work were performed using a DEC 3000/800S workstation acquired through a DEET (Mechanism C) infrastructure grant. Drs A. Igarashi, N. Toshima and T. Shirai were kind enough to provide tabulations of their hyperspherical cross sections.

References

- Archer, B. J., Parker, G. A., and Pack, R. T. (1990). *Phys. Rev. A* **41**, 1303.
Bransden, B. H., and Noble, C. J. (1994). *Adv. At. Mol. Opt. Phys.* **32**, 19.
Brown, C. J., and Humberston, J. W. (1985). *J. Phys. B* **18**, L401.
Charlton, M., Eades, J., Horvath, D., Hughes, R. J., and Zimmerman, C. (1994). *Phys. Rep.* **241**, 67.
Darewych, J. W. (1987). *J. Phys. B* **20**, 5917.
Deutch, B. I., Jacobsen, F. M., Andersen, L. H., Hvelplund, P., Knudsen, H., Holzscheiter, M. H., Charlton, M., and Laricchia, G. (1988). *Phys. Scripta* **T22**, 248.
Deutch, B. I., Charlton, M., Holzscheiter, M. H., Hvelplund, P., Jorgensen, L. V., Knudsen, H., and Laricchia, G., Merrison, J. P., and Poulsen, M. R. (1993). *Hyperfine Inter.* **76**, 153.
Hewitt, R. N., Noble, C. J., and Bransden, B. H. (1990). *J. Phys. B* **23**, 4185.
Higgins, K., and Burke, P. G. (1993). *J. Phys. B* **26**, 4269.
Humberston, J. W. (1984). *J. Phys. B* **17**, 2353.
Humberston, J. W., Charlton, M., Jacobsen, F. M., and Deutch, B. I. (1987). *J. Phys. B* **20**, L25.
Igarashi, A., and Toshima, N. (1994). *Phys. Rev. A* **50**, 232.
Igarashi, A., Toshima, N., and Shirai, T. (1994). *J. Phys. B* **27**, L497; and personal communication.
Kernoghan, A. A., McAlinden, M. T., and Walters, H. R. J. (1994). *J. Phys.* **27**, L543.
McAlinden, M. T., Kernoghan, A. A., and Walters, H. R. J. (1994). *Hyperfine Inter.* **B 89**, 161.
Massey, H. W. S., and Mohr, C. B. O. (1954). *Proc. Phys. Soc. London A* **67**, 695.
Mitroy, J. (1993a). *Aust. J. Phys.* **46**, 751.
Mitroy, J. (1993b). *J. Phys. B* **26**, 4861.
Mitroy, J. (1995). *Aust. J. Phys.* **48**, 645.
Mitroy, J., and Ratnavelu, K. (1995). *J. Phys. B* **28**, 287.
Mitroy, J., and Stelbovics, A. T. (1994a). *J. Phys. B* **27**, 3257.
Mitroy, J., and Stelbovics, A. T. (1994b). *Phys. Rev. Lett.* **72**, 3495.
Mitroy, J., Ratnavelu, K., and Stelbovics, A. T. (1995). *Phys. Rev. Lett.* (in press).
Mott, N. F., and Massey, H. S. W. (1965). 'The Theory of Atomic Collisions' (Oxford University Press).

- Nahar, S. N., and Wadehra, J. M. (1988). *Phys. Rev. A* **37**, 4118.
O'Malley, T. F. (1963). *Phys. Rev.* **130**, 1020.
O'Malley, T. F., Rosenberg, L., and Spruch, L. (1962). *Phys. Rev.* **125**, 1300.
Roy, U., and Mandal, P. (1993). *Phys. Rev. A* **48**, 2952.
Zhou, Y., and Lin, C. D. (1994). *J. Phys. B* **27**, 5065.

Manuscript received 19 April, accepted 14 July 1995